RSC Advances

ROYAL SOCIETY OF CHEMISTRY

www.rsc.org/advances

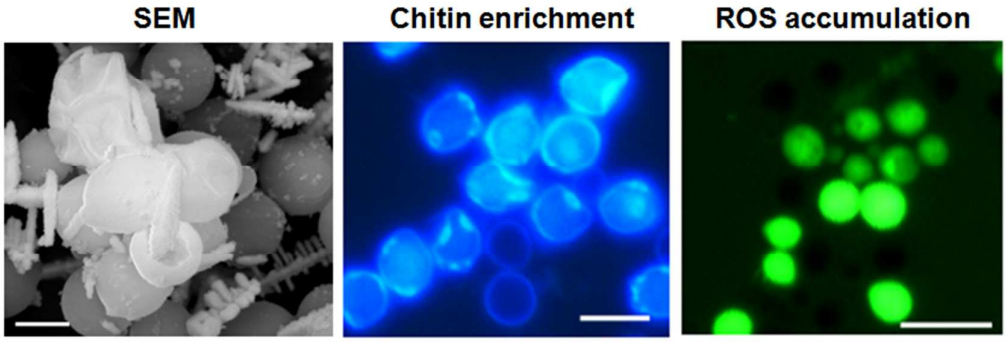

Interaction between PbS nano-dendrites and yeast cells lead to degradation of dendrites, cell wall damage and ROS accumulation.

Interaction between lead sulfide nano-dendrites and *Saccharomyce cerevisiae* is involved in nanotoxicity

Qilin Yu,†[a] Meiqing Sun,†[b] Yu Wang,[a] Mingchun Li*[a] and Lu Liu*[b]

[a]*Key Laboratory of Molecular Microbiology and Technology, Ministry of Education, Department of Microbiology, Nankai University, Tianjin, PR China. E-mail: nklimingchun@163.com; Tel: 86-022-23508506.*

[b]*College of Environmental Science and Engineering, Nankai University, Tianjin, China 300071. E-mail: liul@nankai.edu.cn; Tel: 86-022-23503623.*

† These authors equally contributed to this work.

Abstract

As nano-materials (NMs) are incorporated into ecosystems with increasing amounts, it is urgent to understand the impact of these materials on various biological populations. Lead sulfide (PbS) NMs, such as PbS nano-dendrites and nanoparticles, are important semiconductor materials. While PbS nanoparticles has been implicated to be a risk to organisms, the toxicity of PbS nano-dendrites remains unknown. In this study, we tested the toxicity and related mechanisms of two synthesized PbS nano-dendrites to the model organism *Saccharomyce cerevisiae*. The results demonstrated that the dendrites may interact with the yeast cells, resulting in a degradation of these dendrites and consequent production of nanoparticles. Moreover, this interaction led to a severe damage to the yeast cell wall and intracellular reactive oxygen species (ROS) accumulation, which contribute to the toxicity of the dendrites. These results indicated that the interaction between NMs and the organisms should be included in the studies of nanotoxicity.

1. Introduction

With world-wide advances of nanotechnology and abundant nano-materials (NMs) being incorporated into ecosystems, it is essential and urgent to understand the potential impact of these materials on the environment, especially on living beings.[1-4] Up to now, most of studies focused on the nantoxicity to animals.[5-8] Due to their small sizes and large surface energy, NMs have much higher biological activity than bulk materials.[9,10] Therefore, they may easily enter into cells through free penetration or receptor-mediated endocytosis, and actively interact with cellular components, such as lipids, proteins and genomic DNA.[11-13] These interactions may lead to reactive oxygen species (ROS) accumulation,[14-16] inactivation of protein functions,[17,18] DNA damage,[13] and interference of signaling pathways.[19,20] Consequently, many kinds of NMs produce hazardous effects on the organisms.

Lead sulfide (PbS) NMs, mainly including PbS nano-dendrites and nanoparticles, are important semiconductor materials with a narrow band gap energy and large exciton Bohr radius (18 nm).[21-23] Due to these characteristics, they have been widely used in many fields such as optical switch, photodetectors and solar absorbers.[22, 24-26] Therefore, it is essential to understand their potential toxicity and environmental risks. However, although many lead compounds were demonstrated to have severe impacts on the nervous system, cardiovascular system and kidneys,[27-29] little is known about their biological and environmental effects. Moreover, while a few reports demonstrated that PbS nanoparticles are toxic to fishes and rat neurons,[30-32] the toxicity of PbS nano-dendrites remains unknown.

The fungal community plays a significant role in maintenance of ecological homeostasis, serving as decomposers of organic components to facilitate nutrient recycling and pollutant

detoxification.[33,34] As a particular community, almost all of fungal organisms possess the especial cell wall mainly composed of a flexible network of β-(1,3)-glucan, β-(1,6)-glucan and chitin, glycophosphatidyl-inositol-anchored cell wall proteins (GPI-CWP), and soluble proteins.[35] Unimaginably, the potential hazardous effects of NMs on fungi and related mechanisms are poorly understood. Most recently, we found that PbS nanoparticles showed inhibitory effect on the most important model fungus, *Saccharomyces cerevisiae*, implying a possible risk of PbS NMs to fungal population.[36] In this study, we investigated the toxicity of PbS nano-dendrites to this model organism, and explored possible mechanisms by which these materials caused this toxicity. Our findings revealed their stability-dependent toxicity, which is associated with the interaction between the materials and yeast cells.

2. Experimental

2.1. Synthesis and characterization of PbS nano-dendrites

The PbS nano-dentrites D1 were synthesized as follows. 0.76 g $Pb(AC)_2\ 3H_2O$ and 0.121 g L-cysteine were added into a Teflon-lined autoclave (a volume of 50 mL) and dissolved in 16 mL distilled water by constant strong stirring. 24 mL ethylenediamine was then added to the above solution. The autoclave was sealed and maintained at 180 ℃ for 48 h.[37] The obtained precipitates were centrifuged, washed using deionized water and absolute ethanol several times, and dried at 60 ℃ for 6 h.

To synthesize PbS nano-dendrites D2, 0.445 g Na(AOT) ($C_{20}H_{37}NaO_7S$) was dissolved in 40 mL deionized water. 0.379 g $Pb(AC)_2\ 3H_2O$ and 0.152 g thiourea were then added to the above solution under stirring. The above mixture was then transferred into a Teflon-lined autoclave (a

volume of 50 mL). The autoclave was sealed and maintained at 150 ℃ for 12 h.[38] The products were harvested, washed and dried as described above.

The general morphology of the products was characterized by field-emission scanning electron microscopy (FE-SEM, Nanosem 430, FEI, USA) with an voltage of 0.1-30 kV. Transmission electron microscopy (TEM, Tecnai G^2 F-20, FEI, USA) was also used to observe the morphology of the dendrites prepared in YPD medium (as described below). At least 10 grid samples were observed to evaluate the possible degradation of the materials. The crystal structure and composition of the samples were characterized by X-ray diffraction (XRD, D/max-2500, Japan).

2.2. Preparation of PbS nano-dendrite solutions and Pb^{2+} solutions

The solutions of synthesized PbS nano-dendrites D1 and D2 were prepared in YPD medium with the initial concentration of 10 000 ppm, respectively. The stock solution was then sonicated for 30 min (AS3120, Autoscience, China) and 2-fold diluted using YPD medium, obtaining the following concentrations of nano-dendrites, 160, 320, 640, 1 280 and 2 560 ppm. Pb^{2+} solutions were prepared by dissolving $Pb(NO_3)_2$ in YPD medium, obtaining the solutions with the following Pb^{2+} concentrations, 2, 4, 8, 16 and 32 ppm.

2.3. Strains and growth conditions

Normally, the *S. cerevisiae* strain InvSc1 (Invitrogen, USA) was used in this study. To evaluate the effect of PbS nano-dendrites on expression of the cell wall integrity (CWI) gene *FKS2*, the strain was transformed with the CWI reporting plasmid p2052, in which expression of the gene *LacZ* (encoding β-galactosidase) was governed by the promoter of *FKS2*.[36,39] Yeast cells were overnight

cultured in YPD medium with shaking at 30℃ and suspended in fresh YPD. The suspensions were then mixed with PbS nano-dendrites or Pb^{2+}, and cultured under the same conditions.

2.4. Growth inhibition tests

Growth inhibition by PbS nano-dendrites or Pb^{2+} was tested in glass tubes (a volume of 20 mL). Overnight cultured yeast cells were suspended in fresh YPD medium to an optical density at 600 nm (OD_{600}) of 0.2. 1 mL of cell suspension was added into each tube. To test the inhibitory effect of nano-dendrites, 1 mL of the prepared dendrite solutions with different concentrations were added into the tubes, obtaining 2 mL of the mixtures containing yeast cells with OD_{600} of 0.1 and nano-dendrites with the following concentrations, 0, 80, 160, 320, 640 and 1 280 ppm. For testing the inhibitory effect of Pb^{2+}, 1 mL of cell suspension was mixed with 1 mL of Pb^{2+} solutions, obtaining the mixtures with the following Pb^{2+} concentrations, 0, 1, 2, 4, 8 and 16 ppm. The tubes were cultured with shaking at 30℃ for 12 h. Cells in each tube were counted with haemocytometers, and the percent of growth was calculated as the cell number of each treatment group divided by that of the control (without PbS nano-dendrite and Pb^{2+} treatment) × 100.

2.5. Cell death assays

To evaluate cell death, yeast cells were treated with different concentrations of PbS nano-dendrites for 12 h, harvested and suspended in YPD medium. 100 μL of the suspension was then stained with 1 μL of propidium iodide (PI, dissolved in distilled water, 1 000 ppm, Sigma, USA) for 1 min. The stained cells were then observed using a fluorescence microscope (BX-41, Olympus, Japan). The percent of PI-positive (dead) cells were calculated as the number of PI-positive cells divided

by the total number of cells × 100. At least 30 fields were determined.

2.6. Dissolution of Pb^{2+} from PbS nano-dendrites

To obtain culture supernatant, overnight cultured yeast cells were suspended in YPD medium to an intial OD_{600} of 0.1, and incubated at 30℃ with shaken for 12 h. The cultures were then centrifuged at 12 000 rpm for 10 min to pellet the cells, obtaining culture supernatant. For evaluating dissolved Pb^{2+} in YPD medium or culture supernantant, 1 mL of PbS nano-dendrite solutions (1 280 ppm) were mixed with 1 mL of fresh YPD medium or 1 mL of culture supernatant, obtaining the mixtures containing 640 ppm PbS nano-dendrites. The mixtures were incubated with shaking at 30 ℃ for 12 h and centrifuged at 12,000 rpm for 10 min. Pb^{2+} in the supernatant was detected by ICP-AES (ICP-9000, Jarrell-Ash, USA) and considered as the dissolved Pb^{2+} from the nano-dendrites.

2.7. Observations of yeast cells by SEM and TEM

For scanning electron microscopy (SEM), yeast cells were treated with PbS nano-dendrites (640 ppm) or Pb^{2+} (4 ppm) for 12 h as described above. Cells were harvested, fixed with 2% (v/v) glutaraldehyde, dehydrated with ethanol solutions, and dried in vacuum desiccators. The samples were coated with gold and observed under a scanning electron microscope (QUANTA 200, FEI, Czech). For transmission electron microscopy (TEM), glutaraldehyde-fixed cells were further post-fixed for 2 h with 1% osmium tetroxide solution, dried, and observed by a transmission electron microscope (Tecnai G^2 F-20, FEI, USA).

135 **2.8. Cell wall staining and chitin measurements**

136 For staining the yeast cell wall, cells were treated with PbS nano-dendrites or Pb^{2+} for 12 h as
137 described above. The pellets were then washed, suspended in PBS buffer, and stained with
138 Calcofluor White (CFW, final concentration of 100 ppm, Sigma, USA) for 1 min. Cells were
139 examined by fluorescence microscopy with the blue filter set. To measure chitin contents of the
140 cell wall, CFW-stained cells were washed with PBS three times and added into 96-well
141 fluorescence microplates. The fluorescence density (FLU) of the cells (exitation wave 325 nm,
142 emmision wave 435 nm) were determined with a fluorescence microplate reader (Enspire,
143 Perkinelmer, USA). The cells were also counted with haemocytometers. The relative fluorescence
144 density (RFU) calculated as FLU divided by the number of examined cells.

145

146 **2.9. β- Galactosidase assays**

147 β-Galactosidase assays were performed according to our previous method.[40] Briefly, yeast cells
148 containing the CWI reporting plasmid p2052 were treated with PbS nano-dendrites or Pb^{2+} as
149 described. Cells were then harvested and suspended in 1 mL working Z buffer (60 mM Na_2HPO_4,
150 40 mM NaH_2PO_4, 10 mM KCl, 1 mM $MgSO_4$, 0.027% (v/v) β-mercaptoethanol, pH 7.0). 150
151 μL of suspensions were permeabilized with 20 μL chloroform and 50 μL SDS (0.1%, m/v) at 30℃
152 for 5 min, mixed with 500 μL *O*-nitrophenyl-*β*-D-galactopyranoside (ONPG, 5 000 ppm, BBI,
153 USA), and incubated at 30℃ for certain time (*T*). Reactions were stopped by addition of 500 μL
154 Na_2CO_3 (1 M) when the mixtures turned yellow. Another 50 μL of cell suspensions was diluted
155 with 950 μL of the same buffer, and OD_{600} of the diluted suspensions was determined.
156 Suspensions were centrifuged at 12000 rpm for 10 min, and the optical density of the supernatants

157 at 420 nm (OD_{420}) was determined. Miller units of activity were calculated as (OD_{420}×1000) /
158 (OD_{600}×T×3).

159

160 **2.10. ROS assays**

161 To detect ROS accumulation, the control, PbS nano-dendrite- or Pb^{2+}-treated cells were washed
162 and suspended in PBS buffer. 500 μL of cell suspensions were incubated with 2 μL of 2',
163 7'-dichlorofluorescein diacetate (DCFH-DA, 10 000 ppm, dissolved in PBS) at 30 ℃ for 30 min.
164 The stained cells were harvested, washed and resuspended in PBS buffer. Cells were then
165 examined by fluorescence microscopy with a GFP filter. The percent of ROS-accumulated cells
166 was calculated as the number of DCFH-DA-positive cells divided by the number of total observed
167 cells × 100. At least 30 fields were determined.

168

169 **2.11. Statistical Analysis**

170 Each experiment was performed with three replicates, and the values represent the means ±
171 standard deviation of three experiments. Significant differences between the treatments were
172 determined using one-way ANOVA (P < 0.05). All statistical analyses were performed by
173 Statistical Packages for the Social Sciences (SPSS, Version 20).

174

175 # 3. Results and Discussion

176 **3.1. Morphology and purity of synthesized PbS nano-dendrites**

177 Two PbS nano-dendrites, named D1 and D2, were synthesized in this study. SEM showed that
178 both the synthesized PbS nano-dendrites were in the size with an backbone length of about 2-5 μm.

The arms were about 0.1-1 μm long, with the diameters 40−60 nm for tips and 200−500 nm for the bases (Fig. 1a, Fig. 1b). TEM further showed that both dendrites were composed of regular bases and arms, without any degradation in YPD medium (Fig. 1b).

Figure 1c showed the XRD patterns of the synthesized PbS nano-dendrites D1 and D2. The diffraction patterns distinctly indicated perfect crystallinity of the obtained samples. The reflection peaks of both the dendrites are consistent with the reported values of standard PbS (Card No. JCPDS: 05-0592). No peaks of impurities were detected, revealing the high purity of the synthesized products.

3.2. PbS nano-dendrites showed different inhibitory effects on yeast cells

For investigating the potential toxicity of the PbS nano-dendrites to *S. cerevisiae*, a growth inhibition test was firstly performed. As demonstrated in Figure 2a, after incubated for 12 h, these two kinds of nano-dendrites displayed remarkably different inhibitory effect against *S. cerevisiae* growth. Under the treatment of the dendrites D1, growth of yeast cells was strongly inhibited at the concentrations higher than 320 ppm (IC_{50} = 707.9 ± 26.5 ppm). In contrast, the dendrites D2 showed much weaker inhibitory effect on cell growth, with the IC_{50} > 1 280 ppm.

We further determined whether the inhibitory effect of the dendrites D1 is associated with direct cell damage and consequent cell death caused by these materials. Propidium iodide (PI) staining revealed that only 0.7 % to 1.8% cells were PI-positive (dead) after 12 hours of PbS treatment, and there was no significant difference between the percent of PI-positive cells treated by D1 and that of PI-positive cells treated by D2 (Fig. 2b). This indicated that the strong inhibition of D1 is not attributed to dendrite-caused direct damage to the plasma membrane and related cell death. Other

mechanisms must be included to explain the inhibitory effect of the dendrites D1.

3.3. Pb^{2+} dissolution was not involved in the toxicity of PbS nano-dendrites

For several metal NMs, several evidence suggested that metal ion dissolution contribute to their toxicity.[41-42] Therefore, we evaluated Pb^{2+} dissolution from the tested PbS nano-dendrites in both YPD medium and culture supernatant. ICP-AES assays demonstrated that PbS nano-dendrites D1 released 2.0 to 2.5 ppm Pb^{2+}, while D2 only released 0.6 to 0.8 ppm. Moreover, both D1 and D2 released more Pb^{2+} in culture supernatant than in YPD medium, although there was no significant difference of released Pb^{2+} under the two conditions (Fig. 3a). This implied the positive effect of yeast cells on Pb^{2+} dissolution by cellular metabolic products.

To investigate the possible contribution of Pb^{2+} dissolution to the toxicity of D1, we further tested the effect of Pb^{2+} on yeast growth. After 12 h of incubation, yeast growth was not inhibited by Pb^{2+}, even though its concentration reached to 16 ppm (Fig. 3b). Thus, Pb^{2+} dissolution from D1 (< 4 ppm) is not involved in the dendrites' toxicity.

3.4. Yeast cells led to degradation of PbS nano-dendrites

Since both direct damage to the plasma membrane and Pb^{2+} dissolution do not attribute to the toxicity of the dendrites D1, and the intact dendrites seem not possible to enter the yeast cells, we proposed that an interaction between the nano-dendrites and yeast cells may lead to a degradation of D1, and the produced small PbS nanoparticles resulted in the toxicity. To verify this, we first examined the cell surface and adhering nano-dendrites by SEM. To our expected, after 12 h of co-incubation, the dendrites D1 showed irregular spindle or bud morphology, with their branches

223 broken off from the backbones, implying a severe degradation of D1 caused by yeast cells.
224 Moreover, the degradation resulted in the production of nanoparticles, which abundantly adhered
225 on the cell surface (Fig. 4a). Contrary to D1, the dendrites D2 maintained intact dendritic
226 morphology. Similar to the control cells, D2-treated cells displayed regular smooth surface (Fig.
227 4a). Thus, under the treatment of yeast cells, the dendrites D1, rather than D2, degraded and
228 produced many nanoparticles, which may be associated with the toxicity of D1.

229 Herein, the dendrites D1 degraded much more severely than D2. We proposed that D1 is more
230 sensitive to the metabolic products of yeast cells than D2. Since PbS can be easily attacked by
231 acidic pH, the decrease of pH caused by yeast-produced organic acids may contribute to the
232 sensitivity of D1 to yeast treatment. However, the supernatant pH changes had no obvious
233 difference between the control, the D1-treated group and the D2-treated group (from pH 6.0 to pH
234 5.4-5.6 after 12 h of incubation) (data not shown). This indicated that pH change was not involved
235 in the degradation of D1. Therefore, there may be uncharacterized extracellular metabolic
236 products of the yeast cells that combined with D1 and led to its degradation by chelation force or
237 else. Another possible mechanism of this degradation is that cell wall surface biological
238 macromolecules, especially the cell wall enzymes, catalyzed the degradation of D1. Nevertheless,
239 the degradation mechanisms during the interaction between D1 and yeast cells remain to be
240 elucidated.

241 Entering into cells is a key step for many nanomaterials to cause toxicity.[11, 43] Herein, we further
242 investigated whether the nanoparticles produced by the dendrites D1 entered into yeast cells by
243 TEM. While the control cells and D2-treated cells showed evenly distributed cytoplasm, the
244 D1-treated cells had partially dense areas in the cytoplasm, with abundant dark nanoparticles

accumulated (Fig. 4b). This indicated that the degradation of the dendrites D1 led to the entering of PbS nanoparticles into yeast cells.

As demonstrated above, the PbS dendrites D1 and D2 showed distinct toxicity to yeast cells, which is associated with the difference in their stability when co-incubated with the cells. One explanation to this distinction is the difference in sulfur source during synthesis of these two materials. The sulfur in D1 is supplied by L-cysteine, whereas that in D2 was by thiourea. L-cysteine, an essential amino acid for growth of yeast cells, may led to fine biocompatibility of the synthesized PbS dendrites D1, which may interact with yeast cells more easily and cause more severe toxicity than D2. Another possible explanation is that the dendrites D1 and D2 were synthesized with different templates. The template Na(AOT) may be lead to production of more stable PbS dendrites than ethylenediamine. Although the mechanisms of the toxicity distinction between the materials remain to be investigated, we suggest that stable PbS dendrites should be used to reduce the risk of these nanomaterials to the ecosystem.

3.5. PbS nano-dendrites damaged the yeast cell wall

The cell wall is vital for yeast cells, due to its essential role in cell shape maintenance, defense to osmotic pressure, protection against physical damage and signaling transduction.[44] Damage to this structure has been demonstrated to be involved in the toxicity of PbS nanoparticles.[36] Herein, we further investigated the effect of the PbS nano-dendrites on the cell wall. Although SEM showed that no distinct cell wall damage was observed (Figure 4a), we wonder whether the complicated cell wall construction and functions were affected by nano-dendrites. Chitin, the β-(1,4)-homopolymer of *N*-acetylglucosamine, is one of the important cell wall components

essential for cell shape and morphogenesis.[45] This component was abundantly synthesized under cell wall stress.[46] Here we tested chitin content in the cell wall as an indicator of cell wall damage. Whereas the control yeast cells, together with the D2-treated and Pb^{2+}-treated cells, displayed a regular thin chitin layer, the cells treated with the dendrites D1 showed a much thicker chitin layer (Fig. 5a). Chitin measurement tests further demonstrated that chitin contents of the D1-treated cells were significant higher than the control cells and those cells treated by D2 or Pb^{2+}, revealing an abnormal increase of chitin contents in the cell wall of D1-treated cells (Fig. 5b). This suggested that treatment of D1 caused severe cell wall damage, which led to an enhanced synthesis of cell wall chitin, and this damage is also not attributed by Pb^{2+}.

In yeast cells, cell wall damage will activated a conserved cell wall integrity (CWI) pathway, which led to the up-regulation of CWI genes, such as *FKS2* encoding 1,3-beta-glucan synthase.[47] To evaluate possible activation of the CWI pathway caused by the PbS nan-dendrites, the expression levels of *FKS2* were investigated in the PbS treated yeast cells containing the *FKS2* report plasmid p2052.[39] β-Galactosidase assays revealed that the dendrites D1 caused a significant increase of *FKS2* expression, whereas D2 and Pb^{2+} did not cause this increase (Fig. 5c). Therefore, the CWI pathway was activated in the yeast cells treated by D1, further confirming cell wall damage caused by the dendrites.

3.6. PbS nano-dendrites led to ROS accumulation

ROS generation and consequent oxidative stress are implicated in the toxicity of many NMs after they enter into cells.[14-16] As we demonstrated above, yeast cells caused the degradation of the dendrites D1, which resulted in PbS nanoparticles entering into the cells (Fig. 4a, b). To determine

whether the entered PbS nanoparticles caused toxicity by inducing oxidative stress, we examined intracellular ROS contents in the yeast cells treated by the dendrites. Fluorescence microscopy demonstrated that most of the control cells did not accumulate ROS. While a few D2- and Pb^{2+}-treated cells accumulated ROS compared to the control cells, the dendrites D1 led to the most severe ROS accumulation (Figure 6a). The number of ROS-accumulated cells treated with D1 is 2 to 3 times as much as those treated with D2 or Pb^{2+} (Figure 6b). Thus, the toxicity of the dendrites D1 is supposed to be associated with its effect on ROS generation.

4. Conclusions

In summary, we demonstrated the different toxicity of PbS nano-dendrites to the model fungus, *S. cerevisiae*. Even though the intact PbS nano-dendrites seem impossible to enter the yeast cells and cause toxicity, the synthesized dendrites D1 may interact with the yeast cells, resulting in a degradation of the dendrites and consequent production of nanoparticles. This interaction led to a severe damage to the yeast cell wall and intracellular ROS accumulation, which contribute to the toxicity of the PbS nano-dendrites. These results indicated that the interaction between NMs and the organisms should be included in the studies of nanotoxicity. Moreover, this study revealed that the stability of PbS NMs (or other NMs) is an important factor affecting their toxicity. To reduce the risk of NMs to the ecosystem, their stability should be paid attention in application.

Acknowledgements

We thank Professor David E. Levin (Boston University, USA) for friendly providing the plasmid p2052. We also thank Jiatong Chen and Ping Zhang for fluorescence microscopy. This work was

supported by National Natural Science Foundation of China (Grant 21271108, 81171541, 81373039), Natural Science Foundation of Tianjin (Grant 13JCYBJC20700), Ministry of Science and Technology of China (Grant 2014CB932001), Tianjin Municipal Science and Technology Commission (Grant 12HZGJHZ01100), and China–U.S. Center for Environmental Remediation and Sustainable Development.

References

1 R. D. Handy, F. von der Kammer, J. R. Lead, M. Hassellov, R. Owen and M. Crane, *Ecotoxicology*, 2008, **17,** 287.

2 V. L. Colvin, *Nat. Biotechnol.*, 2003, **21,** 1166.

3 J. P. Ryman-Rasmussen, M. F. Cesta, A. R. Brody, J. K. Shipley-Phillips, J. I. Everitt, E. W. Tewksbury, O. R. Moss, B. A. Wong, D. E. Dodd, M. E. Andersen and J. C. Bonner, *Nat. Nanotechnol.*, 2009, **4,** 747.

4 Y. H. Bai, Y. Zhang, J. P. Zhang, Q. X. Mu, W. D. Zhang, E. R. Butch, S. E. Snyder and B. Yan, *Nat. Nanotechnol.*, 2010, **5,** 683.

5 C. M. Sayes, A. A. Marchione, K. L. Reed and D. B. Warheit, *Nano Lett.*, 2007,**7,** 2399.

6 A. M. Derfus, W. C. W. Chan and S. N. Bhatia, *Nano Lett.*, 2004, **4,** 11.

7 L. Ye, K. T. Yong, L. Liu, I. Roy, R. Hu, J. Zhu, H. Cai, W. C. Law, J. Liu, K. Wang, Y. Liu, Y. Hu, X. Zhang, M. T. Swihart and P. N. Prasad, *Nat. Nanotechnol.*, 2012, **7,** 453.

8 Y. L. Zhao, Q. L. Wu, Y. P. Li and D. Y. Wang, *RSC Adv.*, 2013, **3**, 5741.

9 L. C. Cheng, X. M. Jiang, J. Wang, C. Y. Chen and R. S. Liu, *Nanoscale*, 2013, **5,** 3547.

10 C. M. Sayes and D. B. Warheit, *Wires. Nanomed. Nanobi*., 2009, **1**, 660.

11 L. Zhang, F. X. Gu, J. M. Chan, A. Z. Wang, R. S. Langer and O. C. Farokhzad, *Clin. Pharmacol. Ther.*, 2008, **83**, 761.

12 Y. Roiter, M. Ornatska, A. R. Rammohan, J. Balakrishnan, D. R. Heine and S. Minko, *Nano Lett*., 2008, **8**, 941.

13 R. K. Shukla, A. Kumar, D. Gurbani, A. K. Pandey, S. Singh and A. Dhawan, *Nanotoxicology*, 2013, **7,** 48.

14 K. N. Yu, T. J. Yoon, A. Minai-Tehrani, J. E. Kim, S. J. Park, M. S. Jeong, S. W. Ha, J. K. Lee, J. S. Kim and M. H. Cho, *Toxicol. in Vitro*, 2013, **27,** 1187.

15 X. L. Cheng, W. Q. Zhang, Y. L. Ji, J. Meng, H. Guo, J. Liu, X. C. Wu and H. Y. Xu, *RSC Adv.*, 2013, **3**, 2296.

16 M. S. Wason, J. Colon, S. Das, S. Seal, J. Turkson, J. H. Zhao and C. H. Baker, *Nanomed.-Nanotechnol.*, 2013, **9,** 558.

17 A. Nel, ; T. Xia, L. M ädler and N. Li, *Science*, 2006, **311,** 622.

18 E. Sanfins, J. Dairou, F. Rodrigues-Lima and J.-Marie Dupret *J. Phys. Conf. Ser.*, 2011, **304,** 012039

19 F. Marano, S. Hussain, F. Rodrigues-Lima, A. Baeza-Squiban and S. Boland, *Arch.Toxicol*., 2011, **85,** 733.

20 J. Rauch, W. Kolch, S. Laurent and M. Mahmoudi, *Chem. Rev.*, 2013**, 113,** 3391.

21 J. L. Machol, F. W. Wise, R. C. Patel and D. B. Tanner, *Phys. Rev. B*, 1993, **48,** 15.

22 L. H. Dong, Y. Chu, Y. Liu, M. Y. Li, F.Y. Yang and L. L. Li. *J. Colloid. Interf. Sci.*, 2006, **301**, 503.

23 M. S. Gaponenko, N. A. Tolstik, A. A. Lutich, A. A. Onushchenko and K. V. Yumashev.

Physica E, 2013, **53,** 63.

24 S. A. McDonald, G. Konstantatos, S. G. Zhang, P. W. Cyr, E. J. D. Klem, L. Levina and E. H. Sargent, *Nat. Mater*., 2005, **4,** 138.

25 X. C. Duan, J. M. Ma, Y. Shen and W. J. Zheng, *Inorg. Chem.*, 2012, **51,** 914.

26 R. Plass, S. Pelet, J. Krueger, M. Gratzel and U. Bach, *J. Phys. Chem. B*, 2002, **106**, 7578.

27 G. Flora, D. Gupta and A. Tiwari, *Interdiscip. Toxicol*., 2012, **5,** 47.

28 D. A. Cory-Slechta, *Otolaryngol. Head. Neck. Surg.*, 1996, **114,** 224.

29 A. E. A. Moneim, M. A. Dkhil and S. Al-Quraishy, *J. Hazard. Mater.*, 2011,**194,** 250.

30 G. Oszlanczi, A. Papp, A. Szabo, L. Nagymajtenyi, A. Sapi, Z. Konya, E. Paulik and T. Vezer, *Inhal. Toxicol*., 2011, **23,** 173.

31 L. Truong, I. S. Moody, D. P. Stankus, J. A. Nason, M. C. Lonergan and R. L. Tanguay, *Arch. Toxicol*., 2011, **85,** 787.

32 Y. H. Cao, H. J. Liu, Q. Z. Li, Q. Wang, W. L. Zhang, Y. P. Chen, D. Wang and Y. Cai, *J. Inorg. Biochem*., 2013,**126,** 70.

33 S. Duarte, C. Pascoal, F. Garabetian, F. Cassio and J. Y. Charcosset, *Appl. Environ. Microb*., 2009, **75,** 6211.

34 V. Prigione, V. Tigini, C. Pezzella, A. Anastasi, G. Sannia and G. C. Varese, *Water Res*., 2008, **42,** 2911.

35 P. Orlean, *Genetics*, 2012, **192,** 775.

36 M. Sun, Q. Yu, M. Hu, Z. Hao, C. Zhang and M. Li, *J. Hazard. Mater.*, 2014, **273**, 7.

37 S. Xiong, B. Xi, D. Xu, C. Wang, X. Feng, H. Zhou and Y. Qian, *J. Phys. Chem. C*, 2007, **111,** 16761.

377 38 C. Zhang, Z. H. Kang, E. H. Shen, E. B. Wang, L. Gao, F. Luo, C. G. Tian, C. L. Wang, Y. Lan,
378 J. X. Li and X. J. Cao, *J. Phys. Chem. B*, 2006, **110,** 184.
379 39 K.Y. Kim, A. W. Truman and D. E. Levin, *Mol. Cell. Biol*., 2008, **28,** 2579.
380 40 Q. L. Yu, H. Wang, N. Xu, X. X. Cheng, Y. Z. Wang, B. A. Zhang, L. J. Xing and M. C. Li,
381 *Microbiology-SGM*, 2012,**158**, 2272.
382 41 P. Borm, F. C. Klaessig, T. D. Landry, B. Moudgil, J. Pauluhn, K. Thomas, R. Trottier and S.
383 Wood, *Toxicol. Sci*., 2006, **90**, 23.
384 42 S. J. Klaine, P. J. J. Alvarez, G. E. Batley, T. F. Fernandes, R. D. Handy, D. Y. Lyon, S.
385 Mahendra, M. J. McLaughlin and J. R. Lead, *Environ. Toxicol. Chem*., 2008, **27**, 1825.
386 43 B. D. Chithrani and W.C.W. Chan, *Nano Lett*., 2007, **7,** 1542.
387 44 G. Lesage and H. Bussey, *Microbiol. Mol. Biol. Rev*., 2006, **70,** 317.
388 45 E. Cabib, D.H. Roh, M. Schmidt, L. B. Crotti and A. Varma, *J. Biol. Chem*., 2001, **276,** 19679.
389 46 B. C. Osmond, C. A. Specht and P. W. Robbins, *Proc. Natl. Acad. Sci. USA*, **1999, 96,** 11206.
390 47 P. Mazur, N. Morin, W. Baginsky, M. el-Sherbeini, J. A. Clemas, J. B. Nielsen and F. Foor, *Mol.*
391 *Cell Biol*., 1995, **15,** 5671.
392

Figure legends

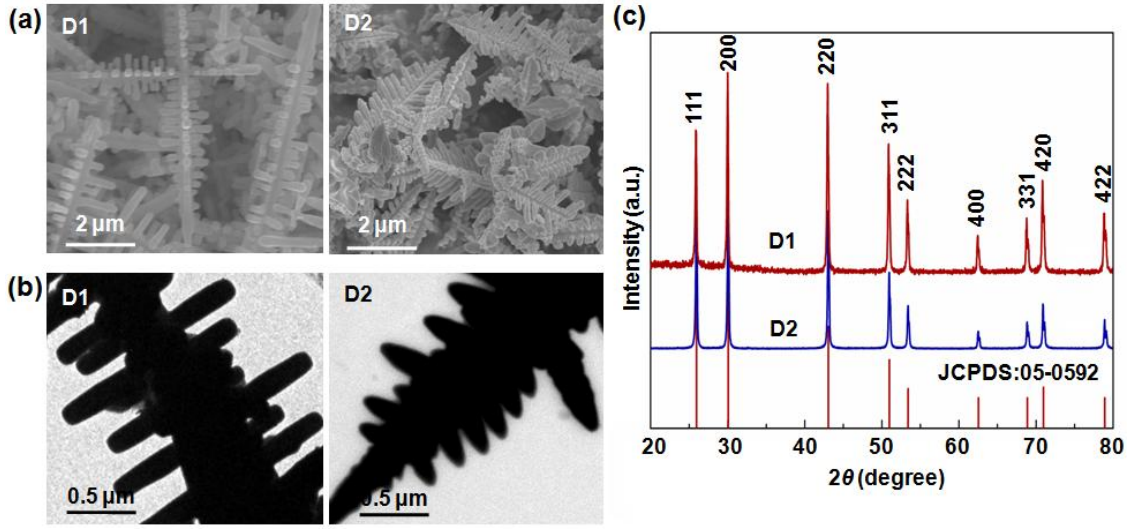

Fig. 1 Characterization of synthesized PbS nano-dendrites. (a) SEM analysis of the synthesized PbS nano-dendrites D1 and D2. (b) TEM analysis of the dendrites D1 and D2. (c) XRD patterns of the dendrites. The standard card of PbS JCPDS: 05-0592 was used.

400

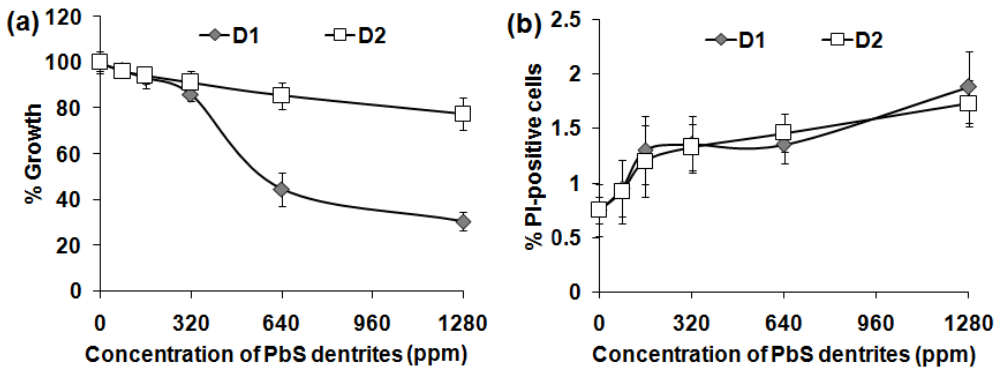

401

402 **Fig. 2** Effect of synthesized PbS nano-dendrites on yeast cell growth (a) and cell damage (b). (a)
403 The overnight cultured yeast cells were treated by PbS nano-dendrites D1 and D2 with the
404 indicated concentrations for 12 h. Cells were then quantified, and the percent of growth were
405 calculated as the number of dendrite-treated cells divided by the number of control cells (without
406 the treatment of the dendrites) × 100. (b) The treated cells were stained with PI and observed using
407 fluorescence microscopy with a RFP filter. The percent of PI-positive cells were calculated as the
408 number of PI-positive (dead) cells divided by the number of total cells × 100. The values represent
409 the means ± standard deviation of three experiments.

410

411

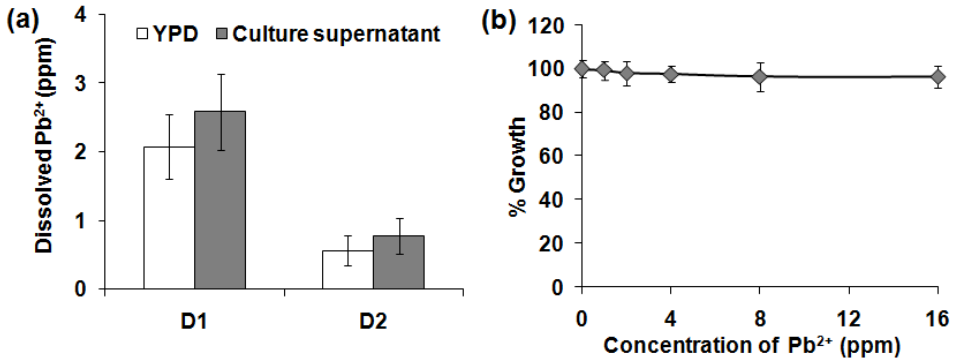

412

413 **Fig. 3** Pb^{2+} dissolution from the PbS nano-dendrites (a) and growth inhibition of Pb^{2+} to yeast

414 cells (b). (a) 640 ppm PbS nano-dendrites were suspended in YPD medium or culture supernatant

415 and incubated with shaking for 12 h. The suspensions were then centrifuged to pellet the materials,

416 and Pb^{2+} contents in the supernatant were determined by ICP-AES. (b) Yeast cells were cultured

417 with shaking for 12 h in YPD medium containing Pb^{2+} with the indicated concentrations. Cells

418 were then quantified, and the percent of growth were calculated. The values represent the means ±

419 standard deviation of three experiments.

420

421

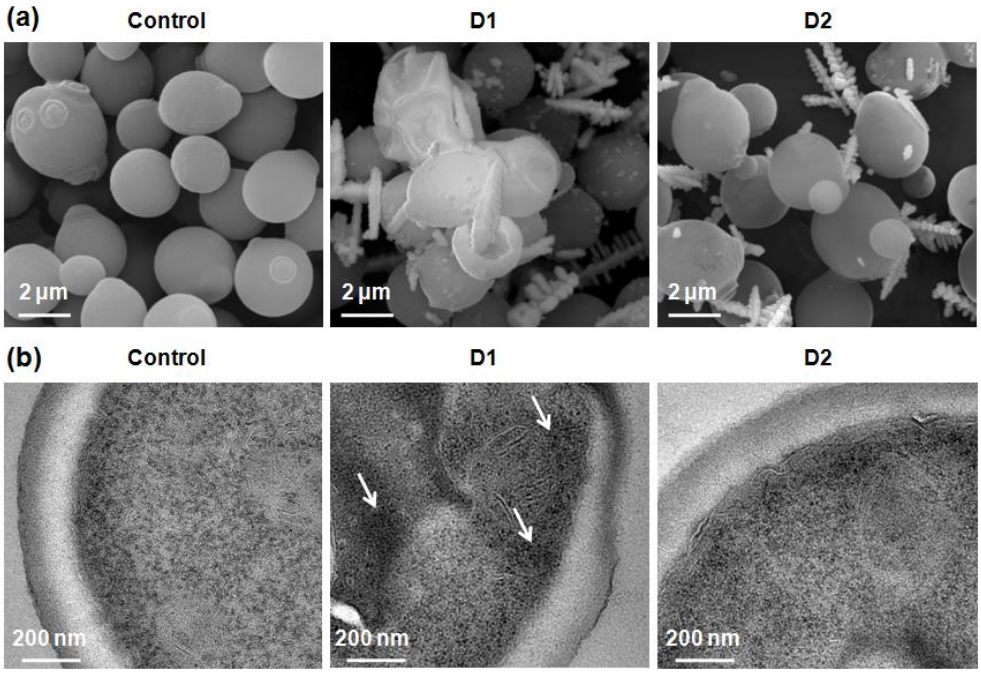

422

423 **Fig. 4** SEM (a) and TEM (b) observations for interacting PbS nano-dendrites and yeast cells. (a)

424 The dendrites (640 ppm) and yeast cells were co-incubated with shaking for 12 h, harvested, fixed,

425 and dried. The samples were then examined using SEM. (b) The fixed cells were cut and observed

426 using TEM. The white arrows in (b) indicated accumulation of PbS nanoparticles.

427

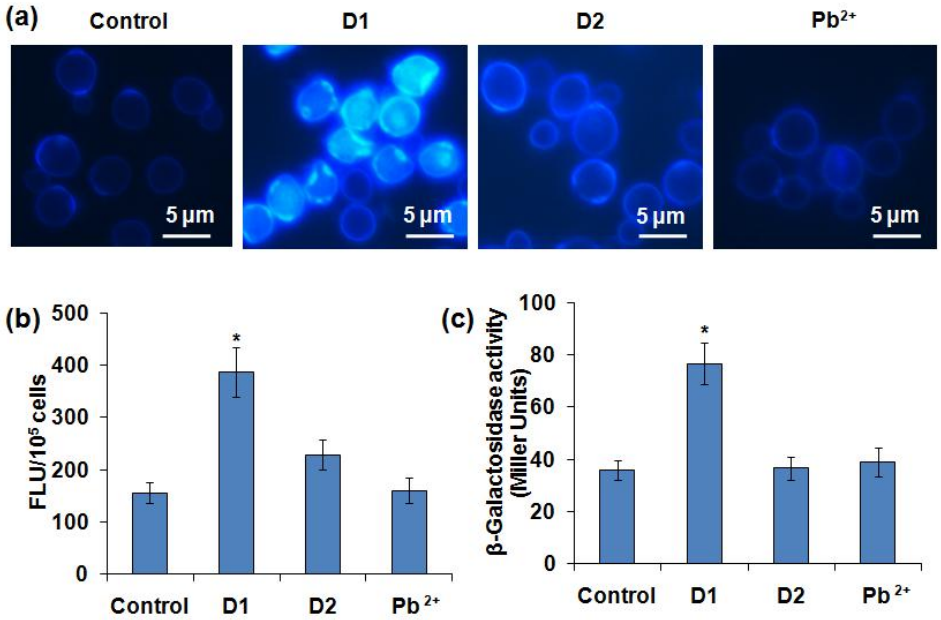

Fig. 5 Chitin contents and expression levels of the CWI gene *FKS2* under the treatment of PbS nano-dendrites and Pb^{2+}. (a) Yeast cells were treated with 640 ppm PbS nano-dendrites D1, D2 or 4 ppm Pb^{2+} for 12 h, stained with CFW, and observed by fluorescence microscopy with a DAPI filter. (b) The fluorescence densities of CFW-stained cells were determined by a fluorescence microplate reader to evaluate chitin contents in the cell wall. (c) The yeast cells containing the CWI reporting plasmid p2052 were treated with D1, D2 or Pb^{2+} as described above, and β-galactosidase activity was determined. The values represent the means ± standard deviation of three experiments. Identical letters indicate no statistical differences among treatments ($P < 0.05$).

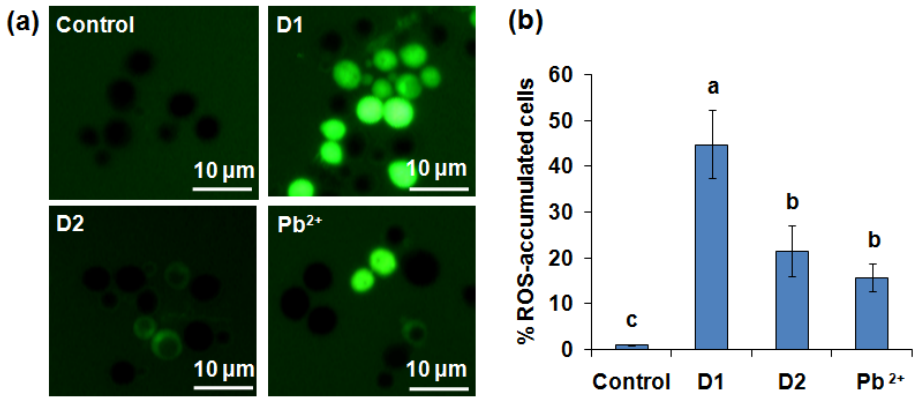

Fig. 6 ROS accumulation in PbS nano-dendrite-treated yeast cells. (a) Yeast cells were treated with D1, D2 or Pb^{2+} as described above, stained with DCFH-DA, and observed by fluorescence microscopy with a GFP filter. (b) The ROS-accumulated (DCFH-DA-positive) cells were quantified, and the percent of ROS-accumulated cells were calculated as the number of ROS-accumulated cells divided by the number of total cells × 100. At least 30 fields were determined. The values represent the means ± standard deviation. Identical letters indicate no statistical differences among the treatments ($P < 0.05$).